

GENERAL FRAMEWORK FOR DISCRETE SURFACE RICCI FLOW

MIN ZHANG, REN GUO, WEI ZENG, FENG LUO, SHING-TUNG YAU,
AND XIANFENG GU

ABSTRACT. Ricci flow deforms the Riemannian metric proportionally to the curvature, such that the curvature evolves according to a heat diffusion process and eventually becomes constant everywhere. Ricci flow has demonstrated its great potential by solving various problems in many fields, which can be hardly handled by alternative methods so far.

This work introduces the unified theoretic framework for discrete Surface Ricci Flow, including all common schemes: Thurston's Circle Packing, Tangential Circle Packing, Inversive Distance Circle Packing and Discrete Yamabe. Furthermore, this work also introduces a novel scheme, virtual radius circle packing, under the unified framework. This work gives explicit geometric interpretation to the discrete Ricci energy for all the schemes, and Hessian of the discrete Ricci energy for schemes with Euclidean back ground geometry.

The unified frame work deepen our understanding to the the discrete surface Ricci flow theory, and inspired us to discover the new schemes, improved the flexibility and robustness of the algorithms, greatly simplified the implementation and improved the debugging efficiency. Experimental results shows the unified surface Ricci flow algorithms can handle general surfaces with different topologies, and is robust to meshes with different qualities, and effective for solving real problems.

1. INTRODUCTION

Ricci flow was introduced by Hamilton for the purpose of studying low dimensional topology. Ricci flow deforms the Riemannian metric proportional to the curvature, such that the curvature evolves according to a heat diffusion process, and eventually becomes constant everywhere. In pure theory field, Ricci flow has been used for the proof of Poincaré's conjecture. In engineering fields, surface Ricci flow has been broadly applied for tackling many important problems, such as parameterization in graphics [23], deformable surface registration in vision [41], manifold spline construction in geometric modeling [15] and cancer detection in medical imaging [40].

Suppose (S, \mathbf{g}) is a metric surface, according to the Gauss-Bonnet theorem, the total Gaussian curvature $\int_S K$ equals to $2\pi\chi(S)$, where K is the Gaussian curvature, $\chi(S)$ the Euler characteristics of S . Ricci flow deforms the Riemannian metric conformally, namely, $\mathbf{g}(t) = e^{2u(t)}\mathbf{g}(0)$, where $u(t) : S \rightarrow \mathbb{R}$ is the conformal factor. The Ricci flow can be written as

$$(1.1) \quad \frac{du(t)}{dt} = -K(t).$$

Surface Ricci flow implies the celebrated surface uniformization theorem as shown in Fig.1. Surface Ricci flow is the negative gradient flow Ricci energy. Ricci flow a

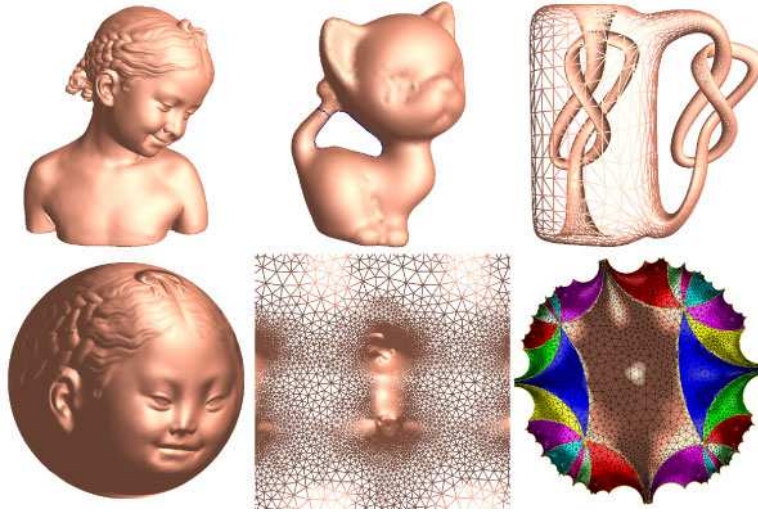


FIGURE 1. Uniformization for closed surfaces by Ricci flow.

powerful tool for designing Riemannian metrics using prescribed curvatures, which has great potential for many applications in engineering fields.

Conformal metric deformation transforms infinitesimal circles to infinitesimal circles. This inspired Thurston to develop the idea of *circle packing* [37]. Intuitively, one approximates the surface by a triangular polyhedron (a triangle mesh), covers each vertex a disk with finite size (a cone), and deforms the disk radii preserving the combinatorial structure of the triangulation and the intersection angles among the circles. This deformation simulates the smooth conformal mapping with very high fidelity. The discrete version of surface Ricci flow has been established based on the circle packing method.

Historically, many schemes of circle packing or circle pattern have been invented. In this work, we focus on the most common ones, including tangential circle packing, Thurston's circle packing, inversive distance circle packing, discrete Yamabe flow. The first three schemes can be unified by the inversive distance circle packing. Furthermore, a novel scheme *virtual radius circle packing* will be introduced. On the other hand, each triangle on the mesh can be treated as a spherical, Euclidean or a hyperbolic triangle. Accordingly, we say the triangle mesh has spherical \mathbb{S}^2 , Euclidean \mathbb{E}^2 or hyperbolic \mathbb{H}^2 background geometry. Therefore, this work focus on three main schemes, (inversive distance circle packing, Yamabe flow and virtual radius circle packing), with three background geometries, (\mathbb{S}^2 , \mathbb{E}^2 , \mathbb{H}^2). There are 9 combinations in total.

All the schemes were invented and developed individually in the past. This work seeks a coherent theoretic framework, which can unify all the existing schemes, and predicts undiscovered ones. In theory, this effort leads to deeper understandings of discrete surface Ricci flow and approaches for further generalization. In practice, the theoretic discovery of virtual radius circle packing gives novel computational algorithm; the mixed schemes improves the flexibility; the unified framework greatly simplifies the implementation; the geometric interpretation helps people to memorize and debug the algorithms.

The theoretic results of the current work can be briefly summarized as follows. We use $(\Sigma, \gamma, \eta, \epsilon)$ to represent a circle packing with background geometry \mathbb{S}^2 , \mathbb{E}^2 and \mathbb{H}^2 , where Σ is the triangulation, γ is the vertex circle radii, η is a function defined on the edges, which gives discrete conformal structure, ϵ is constant in $\{+1, 0, -1\}$, representing inversive distance circle packing, Yamabe flow or virtual radius circle packing respectively. The discrete conformal factor u is defined on vertices,

$$u_i = \begin{cases} \log \gamma_i & \mathbb{E}^2 \\ \log \tanh \frac{\gamma_i}{2} & \mathbb{H}^2 \\ \log \tan \frac{\gamma_i}{2} & \mathbb{S}^2 \end{cases}$$

The Riemannian metric is represented as edge lengths, which is determined by the circle packing,

$$\begin{aligned} l_{ij}^2 &= 2\eta_{ij}e^{u_i+u_j} + \epsilon(e^{2u_i} + e^{2u_j}) & \mathbb{E}^2 \\ \cosh l_{ij} &= \frac{4\eta_{ij}e^{u_i+u_j} + (1+\epsilon e^{2u_i})(1+\epsilon e^{2u_j})}{(1-\epsilon e^{2u_i})(1-\epsilon e^{2u_j})} & \mathbb{H}^2 \\ \cos l_{ij} &= \frac{-4\eta_{ij}e^{u_i+u_j} + (1-\epsilon e^{2u_i})(1-\epsilon e^{2u_j})}{(1+\epsilon e^{2u_i})(1+\epsilon e^{2u_j})} & \mathbb{S}^2 \end{aligned}$$

The edge lengths determine the corner angles by different cosine laws. The vertex curvature K is defined as angle deficit, such that discrete Gauss-Bonnet holds. For all 9 schemes, the discrete surface Ricci flow has exactly the same formula as the smooth case:

$$\frac{du_i(t)}{dt} = -K_i(t),$$

which is the negative gradient flow of the discrete Ricci energy

$$E_\Sigma(u_1, u_2, \dots, u_n) = \int^{(u_1, u_2, \dots, u_n)} \sum_i K_i du_i,$$

The Ricci energy for the whole mesh can be decomposed as the energy on each face. Assume Σ is closed,

$$E_\Sigma = 2\pi \sum_i u_i - \sum_{\Delta \in \Sigma} E_\Delta$$

where $\Delta = [v_i, v_j, v_k]$ is a face of Σ ,

$$E_\Delta(u_i, u_j, u_k) = \int^{(u_i, u_j, u_k)} \theta_i du_i + \theta_j du_j + \theta_k du_k.$$

The geometric meaning of E_Δ is the volume of a generalized hyperbolic tetrahedron, which is completely determined by (u_i, u_j, u_k) and $(\eta_{ij}, \eta_{jk}, \eta_{ki})$. Furthermore, for all 9 schemes, the Hessian of Ricci energy has the same form

$$\frac{\partial(\theta_i, \theta_j, \theta_k)}{\partial(u_i, u_j, u_k)} = \frac{-1}{2A} L \Theta L^{-1} D,$$

where the matrices L , Θ and D has similar structure as shown in Eqn. 5.5, Eqn. 5.6 and Eqn. 5.7.

Furthermore, the Hessian matrix has explicit geometric interpretation in \mathbb{E}^2 case. One can treat the circle packing (Σ, γ) as a power triangulation, which has a dual power diagram $\bar{\Sigma}$. Each edge $e_{ij} \in \Sigma$ has a dual edge $\bar{e} \in \bar{\Sigma}$, then

$$(1.2) \quad \frac{\partial K_i}{\partial u_j} = \frac{\partial K_j}{\partial u_i} = -\frac{|\bar{e}_{ij}|}{|e_{ij}|}, \quad \frac{\partial K_i}{\partial u_i} = -\sum_j \frac{\partial K_i}{\partial u_j}.$$

If the triangulation is power Delaunay, then the Hessian matrix is positive definite, the Ricci energy is convex. In general, the Ricci energies for \mathbb{E}^2 and \mathbb{H}^2 cases are convex. This implies the curvature mapping from the conformal factor to Gaussian curvature is locally bijective, which is called local rigidity. The global rigidity has been established for Thurston's circle packing and Yamabe flow with surgeries.

1.1. **Contributions.** This work has the following contributions:

- (1) this work introduces a novel scheme for discrete surface Ricci flow: virtual radius circle packing, which is naturally deduced from our unification work.
- (2) this work establishes a unified framework for discrete surface Ricci flow, which covers most existing schemes: tangential circle packing, Thurston's circle packing, inversive distance circle packing, discrete Yamabe flow and virtual radius circle packing, with Spherical, Euclidean and hyperbolic background geometry.
- (3) this work gives explicit geometric interpretation to the discrete Ricci energy for all the schemes.
- (4) this work gives explicit geometric interpretation to the Hessian of the discrete Ricci energy for schemes with Euclidean background geometry.

The paper is organized as follows: section 2 briefly reviews the most related theoretic works; section 3 focuses on the smooth surface Ricci flow theory; section 4 explains the discrete surface Ricci flow theory, including all schemes with all background geometries, in a unified way; section 6 reports our implementation based on the unified framework; and the paper is concluded in section 7, which points out future research directions. Finally, in the appendix 7, we give the implementation details and reorganize all the formulae.

2. PREVIOUS WORKS

Ricci flow conformally deforms the Riemannian metrics, such that during the flow the infinitesimal circles are preserved. This phenomenon inspired Thurston to develop the circle packing method. In his work on constructing hyperbolic metrics on 3-manifolds, Thurston [37] studied a Euclidean (or a hyperbolic) circle packing on a triangulated closed surface with prescribed intersection angles. His work generalizes Koebe's and Andreev's results of circle packing on a sphere [3, 4, 24]. Thurston conjectured that the discrete conformal mapping based on circle packing converges to the smooth Riemann mapping when the discrete tessellation becomes finer and finer. Thurston's conjecture has been proved by Rodin and Sullivan [32]. Chow and Luo established the intrinsic connection between circle packing and surface Ricci flow [10].

The rigidity for classical circle packing was proved by Thurston [37], Marden-Rodin [30], Colin de Verdière [11], Chow-Luo [10], Stephenson [36], and He [22]. Bowers-Stephenson [6] introduced inversive distance circle packing which generalizes Andreev-Thurston's intersection angle circle packing. See Stephenson [36] for more information. Guo gave a proof for local rigidity [19]. Luo gave a proof for global rigidity in [28]. Luo studied the combinatorial Yamabe problem for piecewise flat metrics on triangulated surfaces [26]. Springborn, Schröder and Pinkall [35] considered this combinatorial conformal change of piecewise flat metrics and found an explicit formula of the energy function. Glickenstein [12, 13] studied the combinatorial Yamabe flow on 3-dimensional piecewise flat manifolds. Recently

Glickenstein [14] set the theory of combinatorial Yamabe flow of piecewise flat metric in a broader context including the theory of circle packing on surfaces. Combinatorial Yamabe flow on hyperbolic surfaces with boundary has been studied by Guo in [18]. The existence of the solution to Yamabe flow with topological surgeries has been proved recently in [16], which shows the mapping between conformal factor and the curvature is a diffeomorphism.

The variational approach to circle packing was first introduced by Colin de Verdière [11]. Since then, many works on variational principles on circle packing or circle pattern have appeared. For example, see Brägger [39], Rivin [31], Leibon [25], Chow-Luo [10], Bobenko-Springborn [5], Guo-Luo [20], and Springborn [34]. Variational principles for polyhedral surfaces including the topic of circle packing were studied systematically in Luo [27]. Many energy functions are derived from the cosine law and its derivative. Tangent circle packing is generalized to tangent circle packing with a family of discrete curvature. For exposition of this work, see also Luo-Gu-Dai [29].

3. SMOOTH SURFACE RICCI FLOW

This section briefly reviews the fundamental concepts and theorems related to surface Ricci flow. Detailed discussion on Ricci flow on general Riemannian manifolds can be found in [9]. Advanced topics on differential geometry related to Yamabe equations can be found in [33].

3.1. Isothermal Coordinates and Gauss-Bonnet Theorem. Given a metric surface, one can choose *isothermal coordinates* to facilitate geometric computations, as shown in Fig. 2. Most differential operators, such as gradient and Laplace-Beltrami operators, have the simplest form under isothermal coordinates.



FIGURE 2. Isothermal coordinate system on the Stanford bunny surface. The mapping from the surface to the parameter plane is conformal, which preserves angles and infinitesimal circles

Definition 3.1 (Isothermal Coordinates). On a surface S with a Riemannian metric \mathbf{g} , a local coordinates system (u, v) is an isothermal coordinate system, if

$$(3.1) \quad \mathbf{g}(u, v) = e^{2\lambda(u,v)}(du^2 + dv^2),$$

where $\lambda : S \rightarrow \mathbb{R}$ is a function defined on the surface, and called conformal factor.

Isothermal coordinates on metric surfaces always exist, which can be proved either using surface Ricci flow or quasi-conformal mapping. In the later part, we give a proof by solving a Beltrami equation. An elementary proof can be found in Chern's work [7].

Theorem 3.2 (Existence of Isothermal Coordinates). *Let (S, \mathbf{g}) be a compact orientable surface, then every point of S has a neighborhood whose local coordinates are isothermal parameters.*

Under the isothermal coordinates, the Gaussian curvature can be formulated as

$$(3.2) \quad K(u, v) = -e^{-2\lambda(u, v)} \left(\frac{\partial^2}{\partial u^2} + \frac{\partial^2}{\partial v^2} \right) \lambda = -\Delta_{\mathbf{g}} \lambda,$$

where the Laplace-Beltrami operator is

$$\Delta_{\mathbf{g}} = e^{-2\lambda(u, v)} \left(\frac{\partial^2}{\partial u^2} + \frac{\partial^2}{\partial v^2} \right).$$

The Gauss-Bonnet theorem claims that although the Gauss curvature is determined by the Riemannian metric, the total curvature is solely determined by the surface topology.

Theorem 3.3 (Gauss-Bonnet). *Suppose S is a compact two-dimensional Riemannian manifold with piecewise-smooth boundary ∂S . Let K be the Gaussian curvature, k_g the geodesic curvature of ∂S , and $\theta_k, k = 1, 2, \dots, n$ be the exterior angles of ∂S . Then*

$$\int_S K dA + \int_{\partial S} k_g ds + \sum_{k=1}^n \theta_k = 2\pi \chi(S),$$

where $\chi(S)$ is the Euler characteristics of the surface.

3.2. Yamabe Problem. Suppose S is a surface with a Riemannian metric \mathbf{g} , which induces Gauss curvature K and geodesic curvature k_g on the boundary. Let

$$\bar{\mathbf{g}} = e^{2\lambda} \mathbf{g}$$

be another metric conformal to the original one, which induces Gauss curvature \bar{K} and geodesic curvature \bar{k}_g . Then the relations between Gaussian curvature associated to a conformal change of metric are

$$\begin{aligned} \bar{K} &= e^{-2\lambda} (K - \Delta_{\mathbf{g}} \lambda), \\ \bar{k}_g &= e^{-\lambda} (k_g - \partial_{\mathbf{n}, \mathbf{g}} \lambda). \end{aligned}$$

Given (S, \mathbf{g}) and the prescribed curvature, \bar{K} and \bar{k}_g , compute the conformal factor λ . Surface Yamabe problem can be solved using surface Ricci flow.

3.3. Surface Ricci Flow. Given an n dimensional Riemannian manifold M with metric tensor $\mathbf{g} = (g_{ij})$, the normalized Ricci flow is defined by the geometric evolution equation

$$\partial_t \mathbf{g}(t) = -2Ric(\mathbf{g}(t)) + \rho \mathbf{g}(t).$$

where Ric is the Ricci curvature tensor and ρ is the mean value of the scalar curvature

$$\rho = \frac{2}{n} \frac{\int_M R_{\mathbf{g}} d\mu_{\mathbf{g}}}{\int_M d\mu_{\mathbf{g}}},$$

where $R_{\mathbf{g}}$ and $\mu_{\mathbf{g}}$ are the scalar curvature and the volume element with respect to the evolving metric $\mathbf{g}(t)$, respectively. Recall that a one-parameter family of

metrics $\{\mathbf{g}(t)\}$, where $t \in [0, T)$ for some $0 < T \leq \infty$ is called a solution to the normalized Ricci flow if it satisfies the above equation at all $p \in M$ and $t \in [0, T)$.

In two dimensions, the Ricci curvature for a metric \mathbf{g} is equal to $\frac{1}{2}R\mathbf{g}$, where R is the scalar curvature (or twice the Gauss curvature). Therefore, the normalized Ricci flow equation for surfaces takes the form

$$(3.3) \quad \partial_t \mathbf{g}(t) = (\rho - R(t))\mathbf{g}(t),$$

where ρ is the mean value of the scalar curvature,

$$\rho = \frac{4\pi\chi(M)}{A(0)},$$

where $\chi(M)$ is the Euler characteristic number of M , and $A(0)$ is the total area of the surface M at time $t = 0$.

The normalized Ricci flow preserves the total area, $A(t) = A(0), \forall t > 0$. During the Ricci flow (Eqn. 3.3), the metric deforms conformally, $\mathbf{g}(t) = e^{2\lambda(t)}\mathbf{g}(0)$, the conformal factor evolution equation is

$$(3.4) \quad \partial_t \lambda = \frac{1}{2}(\rho - R), \quad \lambda(0) = 0,$$

and the curvature evolution equation is

$$(3.5) \quad \partial_t R = \Delta_{g(t)} R + R(R - \rho).$$

Hamilton [21] and Chow [8] proved the convergence of surface Ricci flow.

Theorem 3.4 (Hamilton [21]). *Let (M^2, g_0) be compact. If $\rho \leq 0$, or if $R(0) \geq 0$ on all of M^2 , then the solution to (3.3) exists for all $t \geq 0$ and converges to a metric of constant curvature.*

Theorem 3.5 (Chow [8]). *If g_0 is any metric on \mathbb{S}^2 , then its evolution under (Eqn. 3.3) develops positive scalar curvature in finite time, and hence by Theorem 3.4 converges to the round metric as t goes to ∞ .*

Surface Ricci flow implies the celebrated surface uniformization theorem.

Theorem 3.6. *Suppose (S, \mathbf{g}) is a compact, there is a function $\lambda : S \rightarrow \mathbb{R}$, such that $e^{2\lambda}\mathbf{g}$ induces constant Gaussian curvature. If the Euler characteristics of S $\chi(S)$ is positive, zero or negative, the constant is $+1, 0, -1$ respectively.*

Namely, as shown in Fig. 1, any closed metric surface can be conformally mapped to the unit sphere \mathbb{S}^2 , the Euclidean plane \mathbb{E}^2 or hyperbolic plane \mathbb{H}^2 . Similarly, surfaces with boundaries can be mapped to one of these three canonical spaces with circular holes (the so-called circle domains), as shown in Fig. 3.

4. DISCRETE SURFACE RICCI FLOW

This section systematically introduces the discrete surface Ricci flow theory. The whole theory is explained using the variational principle on discrete surfaces based on derivative cosine law [29].

Ricci flow conformally deforms the Riemannian metrics, such that during the flow the infinitesimal circles are preserved. This phenomenon inspired Thurston to develop the circle packing method. In his work on constructing hyperbolic metrics on 3-manifolds, Thurston [37] studied a Euclidean (or a hyperbolic) circle packing on a triangulated closed surface with prescribed intersection angles. His work

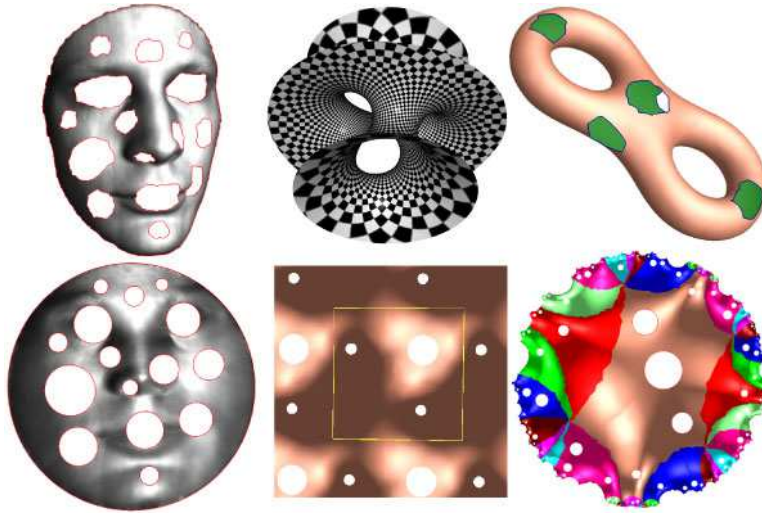


FIGURE 3. Uniformization for surfaces with boundaries

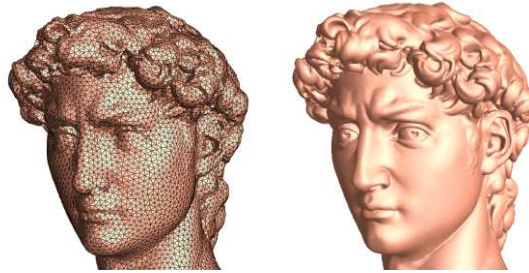


FIGURE 4. Smooth surfaces are approximated by discrete Surfaces

generalizes Koebe's and Andreev's results of circle packing on a sphere [3, 4, 24]. Thurston conjectured that the discrete conformal mapping based on circle packing converges to the smooth Riemann mapping when the discrete tessellation becomes finer and finer. Thurston's conjecture has been proved by Rodin and Sullivan [32]. Chow and Luo established the intrinsic connection between circle packing and surface Ricci flow [10].

4.1. Discrete Surface. In practice, smooth surfaces are usually approximated by discrete surfaces. Discrete surfaces are represented as two dimensional simplicial complexes which are manifolds, as shown in Fig. 4.

Definition 4.1 (Triangular Mesh). Suppose Σ is a two dimensional simplicial complex, furthermore it is also a manifold, namely, for each point p of Σ , there exists a neighborhood of p , $U(p)$, which is homeomorphic to the whole plane or the upper half plane. Then Σ is called a triangular mesh.

If $U(p)$ is homeomorphic to the whole plane, then p is called an interior point; if $U(p)$ is homeomorphic to the upper half plane, then p is called a boundary point.

The fundamental concepts from smooth differential geometry, such as Riemannian metric, curvature and conformal structure, are generalized to the simplicial complex, respectively.

In the following discussion, we use $\Sigma = (V, E, F)$ to denote the mesh with vertex set V , edge set E and face set F . A discrete surface is with Euclidean (hyperbolic or spherical) background geometry if it is constructed by isometrically gluing triangles in \mathbb{E}^2 (\mathbb{H}^2 or \mathbb{S}^2).

Definition 4.2 (Discrete Riemannian Metric). A discrete metric on a triangular mesh is a function defined on the edges, $l : E \rightarrow \mathbb{R}^+$, which satisfies the triangle inequality: on each face $[v_i, v_j, v_k]$,

$$l_{ij} + l_{jk} > l_{ki}, \quad l_{jk} + l_{ki} > l_{ij}, \quad l_{ki} + l_{ij} > l_{jk}.$$

A triangular mesh with a discrete Riemannian metric is called a discrete metric surface.

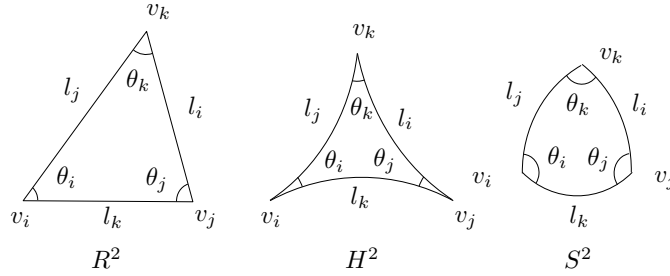


FIGURE 5. Different background geometry, Euclidean, spherical and hyperbolic.

Definition 4.3 (Background Geometry). Suppose Σ is a discrete metric surface, if each face of Σ is a spherical, (Euclidean or hyperbolic) triangle, then we say Σ is with spherical, (Euclidean or hyperbolic) background geometry. We use \mathbb{S}^2 , \mathbb{E}^2 and \mathbb{H}^2 to represent spherical Euclidean or hyperbolic background metric.

Triangles with different background geometries satisfy different cosine laws:

$$\begin{aligned} 1 &= \frac{\cos \theta_i + \cos \theta_j \cos \theta_k}{\sin \theta_j \sin \theta_k} && \mathbb{E}^2 \\ \cos l_i &= \frac{\cos \theta_i + \cos \theta_j \cos \theta_k}{\sin \theta_j \sin \theta_k} && \mathbb{S}^2 \\ \cosh l_i &= \frac{\cosh \theta_i + \cosh \theta_j \cosh \theta_k}{\sinh \theta_j \sinh \theta_k} && \mathbb{H}^2 \end{aligned}$$

The discrete Gaussian curvature is defined as angle deficit, as shown in Fig. 6.

Definition 4.4 (Discrete Gauss Curvature). The discrete Gauss curvature function on a mesh is defined on vertices, $K : V \rightarrow \mathbb{R}$,

$$K(v) = \begin{cases} 2\pi - \sum_i \alpha_i, & v \notin \partial M \\ \pi - \sum_i \alpha_i, & v \in \partial M \end{cases},$$

where α_i 's are corner angles adjacent to the vertex v , and ∂M represents the boundary of the mesh.

The Gauss-Bonnet theorem still holds in the discrete case.

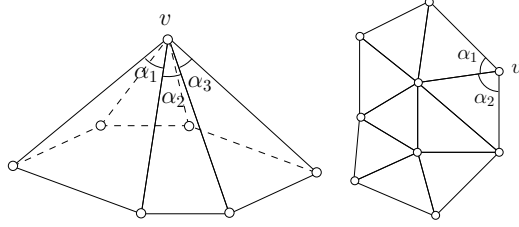


FIGURE 6. Discrete curvatures of an interior vertex and a boundary vertex

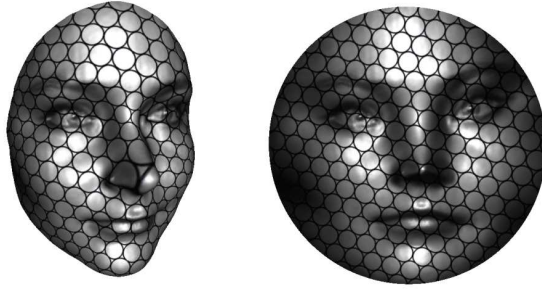


FIGURE 7. Conformal mapping preserves infinitesimal circles.

Theorem 4.5 (Discrete Gauss-Bonnet Theorem). *Suppose Σ is a triangular mesh with Euclidean background metric. The total curvature is a topological invariant,*

$$\sum_{v \notin \partial \Sigma} K(v) + \sum_{v \in \partial \Sigma} K(v) + \epsilon A(\Sigma) = 2\pi \chi(\Sigma),$$

where χ is the characteristic Euler number, and K is the Gauss curvature, $A(\Sigma)$ is the total area, $\epsilon = \{+1, 0, -1\}$ if Σ is with spherical, Euclidean or hyperbolic background geometry.

4.2. Thurston’s Circle Packing Idea. Surface Ricci flow conformally deforms the Riemannian metric, such that infinitesimal circles are mapped to infinitesimal circles, as shown in Fig. 7. This inspires Thurston to develop circle packing idea as shown in Fig. 8. Suppose one wants to compute the Riemann mapping from a planar domain Ω to the unit disk \mathbb{D} . Here we treat the unit disk as the Poincaré disk, namely the Riemannian metric is

$$\mathbf{g} = \frac{dzd\bar{z}}{(1 - z\bar{z})^2}.$$

One can triangulate Ω , and associate each vertex v_i with a circle $C_i = (v_i, \gamma_i)$. For each edge $[v_i, v_j]$, two circles at the end vertices C_i and C_j are tangential to each other. This procedure constructs a circle packing of Ω with hyperbolic background geometry. Then one can deform the circle packing, preserving the combinatorial structure and the tangential relations among the circles, such that the boundary circle radii approach to ∞ , and all interior vertex curvatures are kept to be zeros. This deformation between Ω and \mathbb{D} can be treated as a discrete conformal mapping.

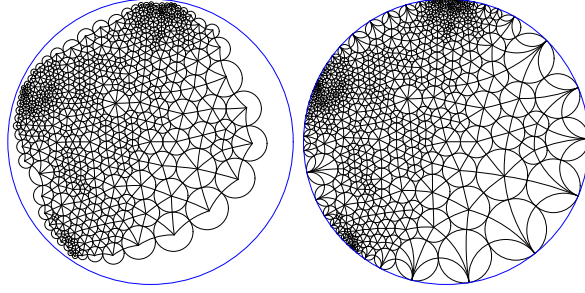


FIGURE 8. Tangential circle packing on the hyperbolic disk.

If the triangulation is subdivided infinite times, the induced discrete conformal mappings converge to the smooth Riemann mapping.

Definition 4.6 (Circle Packing Metric). Suppose $\Sigma = (V, E, F)$ is triangle mesh with spherical, Euclidean or hyperbolic background geometry. Each vertex v_i is associated with a circle with radius γ_i . The circle radius function is denoted as $\gamma : V \rightarrow \mathbb{R}_{>0}$; a function defined on the vertices $\epsilon : V \rightarrow \{+1, 0, -1\}$ is called the *scheme coefficient*; a function defined on edges $\eta : E \rightarrow \mathbb{R}$ is called the *discrete conformal structure*. A circle packing metric is a 4-tuple $(\Sigma, \gamma, \eta, \epsilon)$, the edge length is determined by the 4-tuple.

In the smooth case, changing a Riemannian metric by a scalar function, $\mathbf{g} \rightarrow e^{2u}\mathbf{g}$, is called a conformal metric deformation. The discrete analogy to this is as follows.

Definition 4.7 (Discrete Conformal Equivalence). Two circle packing metrics $(\Sigma_k, \gamma_k, \eta_k, \epsilon_k)$, $k = 1, 2$, are conformally equivalent if $\Sigma_1 = \Sigma_2$, $\eta_1 = \eta_2$, $\epsilon_1 = \epsilon_2$.

The discrete analogy to the concept of conformal factor in the smooth case is

Definition 4.8 (Discrete Conformal Factor). Discrete conformal factor for a circle packing metric $(\Sigma, \gamma, \eta, \epsilon)$ is a function defined on each vertex $\mathbf{u} : V \rightarrow \mathbb{R}$,

$$u_i = \begin{cases} \log \gamma_i & \mathbb{E}^2 \\ \log \tanh \frac{\gamma_i}{2} & \mathbb{H}^2 \\ \log \tan \frac{\gamma_i}{2} & \mathbb{S}^2 \end{cases}$$

The following symmetric relation has fundamental importance.

Lemma 4.9 (Symmetry). *A discrete surface with \mathbb{S}^2 , \mathbb{E}^2 or \mathbb{H}^2 background geometry, and a circle packing metric $(\Sigma, \gamma, \eta, \epsilon)$, then for any pair of vertices v_i and v_j :*

$$(4.1) \quad \frac{\partial K_i}{\partial u_j} = \frac{\partial K_j}{\partial u_i}.$$

Furthermore, the partial derivatives have explicit geometric meaning, which will be explained in details in later sections.

Definition 4.10 (Discrete Surface Ricci Flow). A discrete surface with \mathbb{S}^2 , \mathbb{E}^2 or \mathbb{H}^2 background geometry, and a circle packing metric $(\Sigma, \gamma, \eta, \epsilon)$, the discrete surface Ricci flow is

$$(4.2) \quad \frac{du_i(t)}{dt} = \bar{K}_i - K_i(t),$$

where \bar{K}_i is the target curvature at the vertex v_i .

The discrete surface Ricci flow has exactly the same formula as the smooth counter part 3.3. Furthermore, similar to the smooth case, discrete surface Ricci flow is also variational: the discrete Ricci flow is the negative gradient flow of the discrete Ricci energy.

Definition 4.11 (Discrete Ricci Energy). A discrete surface with \mathbb{S}^2 , \mathbb{E}^2 or \mathbb{H}^2 background geometry, and a circle packing metric $(\Sigma, \gamma, \eta, \epsilon)$, the discrete surface Ricci energy is

$$(4.3) \quad E_\Sigma(u_1, u_2, \dots, u_n) = \int^{(u_1, u_2, \dots, u_n)} \sum_{i=1}^n (\bar{K}_i - K_i) du_i.$$

The desired metric inducing the target curvature \bar{K} is a critical point of the discrete Ricci energy. The symmetry relation 4.1 shows the discrete Ricci energy is well defined. The discrete Ricci energy has explicit geometric meaning as well, which will be further explained later.

Remark 4.12. Suppose $(\Sigma, \gamma, \eta, \epsilon)$ is with \mathbb{E}^2 and \mathbb{H}^2 background geometry, and Σ is a (power) Delaunay triangulation (the power distance is determined by the schemes), then the discrete Ricci energies are convex. The convexity implies the local rigidity, namely the curvature mapping

$$(4.4) \quad \nabla E_\Sigma : (u_1, u_2, \dots, u_n) \rightarrow (K_1, K_2, \dots, K_n)$$

is locally injective.

Remark 4.13. For Thurston's circle packing scheme with both \mathbb{E}^2 and \mathbb{H}^2 background geometry, the admissible spaces of discrete conformal factors are also convex, which implies the global rigidity, namely the curvature mapping 4.4 is a global diffeomorphism. The admissible curvature space is a convex polytope, constrained by a set of linear inequalities.

Remark 4.14. For Yamabe flow scheme with both \mathbb{E}^2 and \mathbb{H}^2 background geometry, if Σ is preserved to be Delaunay during the flow, then the curvature mapping 4.4 is a global diffeomorphism [16],

$$\nabla E_\Sigma : \mathbb{R}^n \cap \left\{ \sum_{i=1}^n u_i = 0 \right\} \rightarrow (-\infty, 2\pi)^n.$$

Remark 4.15. Discrete Ricci flow for surfaces with spherical background geometry in general is not convex, which causes numerical instability. Therefore, in practice, instead of mapping the surface onto the unit sphere, one can map the surface onto the Euclidean plane first using Euclidean Ricci flow, then map the plane to the sphere by the stereo-graphic projection.

5. VARIOUS SCHEMES

In the following, we explain different schemes in details. We only focus on one triangle $[v_i, v_j, v_k]$, with corner angles $\theta_i, \theta_j, \theta_k$, conformal factors u_i, u_j, u_k and edge lengths l_{ij} for edge $[v_i, v_j]$, l_{jk} for $[v_j, v_k]$ and l_{ki} for $[v_k, v_i]$. The Ricci energy of the triangle is

$$(5.1) \quad E(u_i, u_j, u_k) = \int^{(u_i, u_j, u_k)} \theta_i du_i + \theta_j du_j + \theta_k du_k.$$

Under each background geometry \mathbb{E}^2 , \mathbb{H}^2 and \mathbb{S}^2 , there are 5 different schemes: tangential circle packing, Thurston's circle packing, inversive distance circle packing, Yamabe flow and virtual radius circle packing.

5.1. Euclidean Background Geometry.

Edge Length. Given a circle packing metric $(\Sigma, \gamma, \eta, \epsilon)$ The edge length on $[v_i, v_j]$ is given by

$$(5.2) \quad l_{ij}^2 = 2\eta_{ij}\gamma_i\gamma_j + \epsilon_i\gamma_i^2 + \epsilon_j\gamma_j^2.$$

where ϵ is $+1$ for tangential/Thurston's/inversive distance circle packing, 0 for discrete Yamabe flow, -1 for virtual radius circle packing.

Hessian Matrix. The Hessian of the energy function 5.1 is the Jacobian

$$(5.3) \quad \frac{\partial(\theta_i, \theta_j, \theta_k)}{\partial(u_i, u_j, u_k)} = -\frac{1}{2A}L\Theta L^{-1}D,$$

In the following, we use the function $s(x) = x$. In the above formula, A is the triangle area

$$(5.4) \quad A = \frac{1}{2} \sin \theta_i s(l_j) s(l_k),$$

the matrix L

$$(5.5) \quad L = \begin{pmatrix} s(l_i) & 0 & 0 \\ 0 & s(l_j) & 0 \\ 0 & 0 & s(l_k) \end{pmatrix}$$

the matrix Θ

$$(5.6) \quad \Theta = \begin{pmatrix} -1 & \cos \theta_k & \cos \theta_j \\ \cos \theta_k & -1 & \cos \theta_i \\ \cos \theta_j & \cos \theta_i & -1 \end{pmatrix}$$

and

$$(5.7) \quad D = \begin{pmatrix} 0 & \tau(i, j, k) & \tau(i, k, j) \\ \tau(j, i, k) & 0 & \tau(j, k, i) \\ \tau(k, i, j) & \tau(k, j, i) & 0 \end{pmatrix}$$

where $\tau(i, j, k) = \frac{1}{2}(l_i^2 + \epsilon_j\gamma_j^2 - \epsilon_k\gamma_k^2)$.

The formula for Hessian matrix 5.3 can be applied for optimizing the Ricci energy using Newton's method.

Geometric Interpretation. The geometric meaning for the Hessian matrix is as follows. As shown in Fig. 9, the *power* of q with respect to v_i is

$$pow(v_i, q) = |v_i - q|^2 - \epsilon\gamma_i^2.$$

The *power center* o of the triangle satisfies

$$pow(v_i, o) = pow(v_j, o) = pow(v_k, o).$$

The *power circle* C centered at o with radius γ , where $\gamma = pow(v_i, o)$. Therefore, for tangential, Thurston's and inversive distance circle packing cases, the power circle is orthogonal to three circles at the vertices C_i , C_j and C_k ; for Yamabe flow case, the power circle is the circumcircle of the triangle; for virtual radius circle packing, the power circle is the equator of the sphere, which goes through three points $\{v_i + \gamma_i^2 \mathbf{n}, v_j + \gamma_j^2 \mathbf{n}, v_k + \gamma_k^2 \mathbf{n}\}$, where \mathbf{n} is the normal to the plane.

Through the power center, we draw line perpendicular to three edges, the perpendicular feet are w_i, w_j and w_k respectively. The distance from the power center to the perpendicular feet are h_i, h_j and h_k respectively. Then it can be shown easily that

$$(5.8) \quad \frac{\partial \theta_i}{\partial u_j} = \frac{\partial \theta_j}{\partial u_i} = \frac{h_k}{l_k}, \quad \frac{\partial \theta_j}{\partial u_k} = \frac{\partial \theta_k}{\partial u_j} = \frac{h_i}{l_i}, \quad \frac{\partial \theta_k}{\partial u_i} = \frac{\partial \theta_i}{\partial u_k} = \frac{h_j}{l_j},$$

furthermore,

$$(5.9) \quad \frac{\partial \theta_i}{\partial u_i} = -\frac{h_k}{l_k} - \frac{h_j}{l_j}, \quad \frac{\partial \theta_j}{\partial u_j} = -\frac{h_k}{l_k} - \frac{h_i}{l_i}, \quad \frac{\partial \theta_k}{\partial u_k} = -\frac{h_i}{l_i} - \frac{h_j}{l_j}.$$

These two formula induces the formula in Eqn. 1.2.

The geometric interpretation to the discrete Ricci energy in Eqn. 5.1 is the volume of a truncated ideal hyperbolic prism. We use the upper half space model for \mathbb{H}^3 , with Riemannian metric

$$ds^2 = \frac{dx^2 + dy^2 + dz^2}{z^2}$$

the xy-plane is the infinite plane. We draw the triangle on the xy-plane, and draw vertical lines through three vertices, this gives us a prism. Then we through each vertex circle, we either draw a hyperbolic plane (Euclidean hemispheres orthogonal to the xy-plane) or a horosphere, and/or draw a hyperbolic plane through the power circle. The prism is cut off by these hyperbolic planes or horospheres, the volume of the truncated hyperbolic idea tetrahedron is the discrete Ricci energy in Eqn. 5.1. Details are illustrated by Fig. 9.

Suppose on the edge $[v_i, v_j]$, the distance from v_i to the perpendicular foot w_k is d_{ij} , the distance from v_j to w_k is d_{ji} , then $l_{ij} = d_{ij} + d_{ji}$, and

$$\frac{\partial l_{ij}}{\partial u_i} = d_{ij}, \quad \frac{\partial l_{ij}}{\partial u_j} = d_{ji},$$

furthermore

$$d_{ij}^2 + d_{jk}^2 + d_{ki}^2 = d_{ik}^2 + d_{kj}^2 + d_{ji}^2.$$

Tangential Circle Packing. Fig. 9 row (a) shows the tangential circle packing scheme, where circles at the end vertices of each edge are tangential to each other.

$$l_{ij} = \gamma_i + \gamma_j.$$

The truncated hyperbolic tetrahedron is obtained by cutting off the prism by the hyperbolic planes through all the vertex circles and the power circle.

Thurston's Circle Packing. As shown in Fig. 9 row (b), two circles centered at the end vertices of the same edge intersect each other. Assume the intersection angle on edge $[v_i, v_j]$ is ϕ_{ij} , where $0 < \phi_{ij} \in [0, \frac{\pi}{2}]$, which determines the conformal structure coefficient $\eta_{ij} = \cos \phi_{ij}$. Then the edge length is given by

$$l_{ij}^2 = 2 \cos \phi_{ij} \gamma_i \gamma_j + \gamma_i^2 + \gamma_j^2.$$

The tangential circle packing is the special case of this scheme, where each ϕ_{ij} is zero. The construction of the truncated hyperbolic tetrahedron is similar to that of tangent circle packing.

Inversive Distance Circle Packing. As shown in Fig. 9 row (c), this scheme further generalizes Thurston's scheme. On each edge $[v_i, v_j]$, two circles C_i and C_j are separated, the discrete conformal structure coefficient $\eta_{ij} > 1$. The edge length is given by

$$l_{ij}^2 = 2\eta_{ij}\gamma_i\gamma_j + \gamma_i^2 + \gamma_j^2.$$

The construction of the truncated hyperbolic tetrahedron is similar.

Yamabe Flow. As shown in Fig. 9 row (d), the edge length is given by

$$l_{ij}^2 = 2\eta_{ij}\gamma_i\gamma_j,$$

where $\eta_{ij} = \frac{L_{ij}^2}{2}$, L_{ij} is the initial edge length, namely

$$l_{ij} = e^{\frac{u_i}{2}} L_{ij} e^{\frac{u_j}{2}}.$$

The power circle is the circum circle of the triangle. The truncated hyperbolic tetrahedron is constructed as follows: draw a horosphere through the vertices v_i, v_j and v_k , with Euclidean radii γ_i, γ_j and γ_k , and draw a hemisphere through the power circle. The prism is cut off by these horospheres and the hyperbolic plane.

Virtual Radius Circle Packing. As shown in Fig. 9 row (e), the vertex circles are with imaginary radius, the edge length is given by

$$l_{ij}^2 = 2\eta_{ij}\gamma_i\gamma_j - \gamma_i^2 - \gamma_j^2.$$

We vertically lift vertex v_i to p_i , $p_i = v_i + \gamma_i^2 \mathbf{n}$, similarly lift v_j and v_k to p_j and p_k . Draw a hemisphere through p_i, p_j and p_k , orthogonal to the xy -plane. The hemisphere cuts off the prism, the volume of the truncated hyperbolic tetrahedron gives the Ricci energy.

Mixed Scheme. Fig. 10 shows the mixed scheme, which mixes inversive distance circle packing at v_i , virtual radius circle packing v_j and Yamabe flow at v_k , namely $(\epsilon_i, \epsilon_j, \epsilon_k) = (+1, -1, 0)$. The edge length is given by

$$l_k^2 = 2\eta_{ij}\gamma_i\gamma_j + \gamma_i^2 - \gamma_j^2, l_i^2 = 2\eta_{jk}\gamma_j\gamma_k - \gamma_j^2, l_j^2 = 2\eta_{ki}\gamma_k\gamma_i + \gamma_i^2.$$

The power circle is constructed as follows: lift v_j to $p_j = v_j + \gamma_j^2 \mathbf{n}$, draw a hemisphere through v_k and p_j , and its equator is orthogonal to the circle (v_i, γ_i) . The Hessian matrix formulae, Eqn. 5.8 and Eqn. 5.9, still hold. We draw hemispheres from the vertex circle (v_i, γ_i) and the power circle, and a horosphere through v_k with Euclidean radius γ_k , the prism is cut off by these spheres, the volume of the left part is the discrete Ricci energy.

5.2. Hyperbolic Background Geometry. For discrete surface with hyperbolic background geometry, with the circle packing metric $(\Sigma, \gamma, \eta, \epsilon)$, suppose the conformal structure coefficient η is a constant function defined on edges, then for each edge $[v_i, v_j]$, the edge length is given by

$$\cosh l_{ij} = \frac{4\eta_{ij}e^{u_i+u_j} + (1 + \epsilon_i e^{2u_i})(1 + \epsilon_j e^{2u_j})}{(1 - \epsilon_i e^{2u_i})(1 - \epsilon_j e^{2u_j})},$$

where $u_i = \log \tanh \frac{\gamma_i}{2}$ is the discrete conformal factor, ϵ is $+1$ for tangential/Thurston's/inversive distance circle packing, 0 for discrete Yamabe flow and -1 for virtual radius circle packing. The Hessian of the energy function or the Jacobian has similar formula

$$\frac{\partial(\theta_i, \theta_j, \theta_k)}{\partial(u_i, u_j, u_k)} = -\frac{1}{2A} L \Theta L^{-1} D,$$

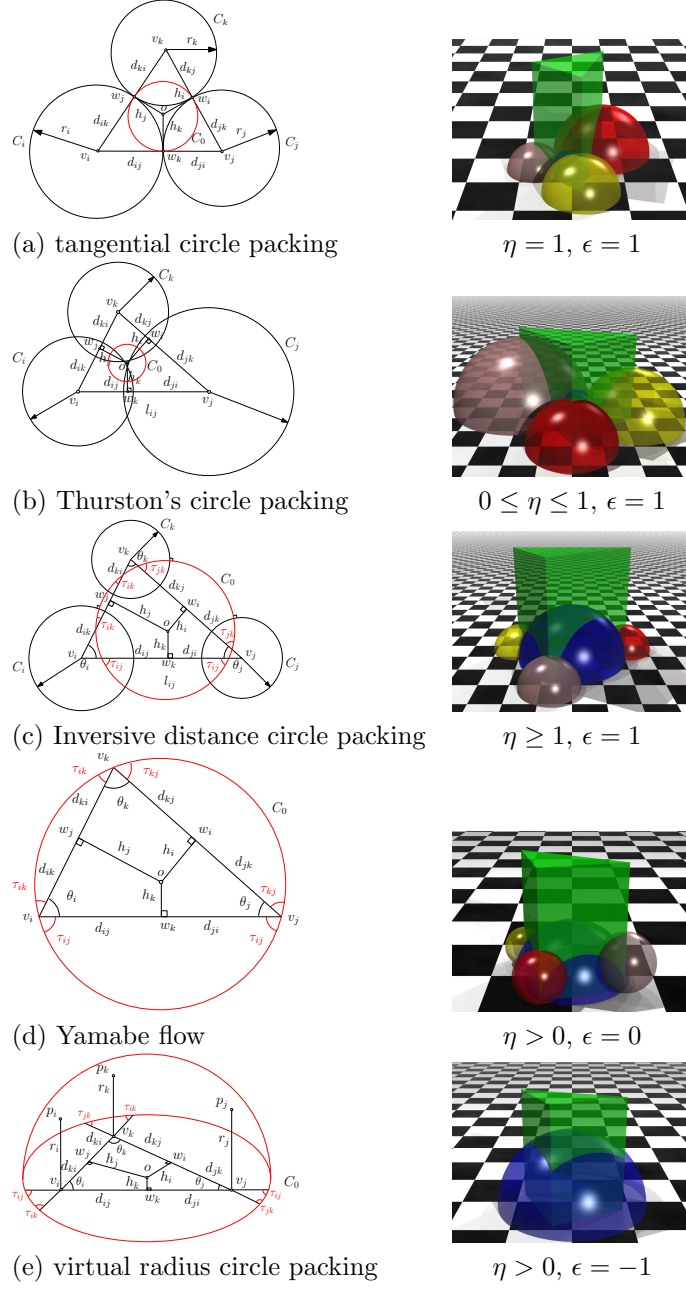


FIGURE 9. Different circle packing schemes

where A and L is similar to those in Eqn. 5.4 and Eqn. 5.5 with $s(x) = \sinh x$, Θ is the same as in Eqn. 5.6, and D is similar to that in Eqn. 5.7 with

$$\tau(i, j, k) = \cosh l_i \cosh^{\epsilon_j} \gamma_j - \cosh^{\epsilon_k} \gamma_k.$$

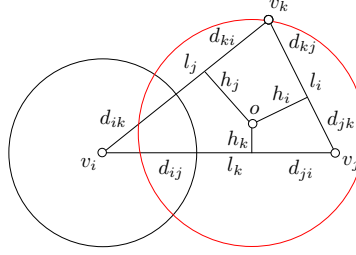


FIGURE 10. Mixed type scheme

Inversive Distance Circle Packing. The tangential and Thurston's circle packings can be unified as inversive distance circle packing. In this scheme ϵ is $+1$, $\eta_{ij} > 0$, the length is given by

$$\cosh l_{ij} = \eta_{ij} \sinh \gamma_i \sinh \gamma_j + \cosh \gamma_i \cosh \gamma_j.$$

As shown in Fig. 14 1st row and 2nd column, the hyperbolic tetrahedron has four hyperideal vertices, each vertex is cut by a hyperbolic plane, such that the top section is a hyperbolic triangle with lengths l_{ij} , l_{jk} and l_{ki} , the "vertical" edge lengths are $-u_i$, $-u_j$ and $-u_k$ respectively. The bottom lengths are λ_{ij} , λ_{jk} and λ_{ki} respectively, where

$$\cosh \lambda_{ij} = \eta_{ij}.$$

Yamabe Flow. In this scheme ϵ is 0 , $\eta_{ij} > 0$, The edge length is given by

$$\sinh \frac{l_{ij}}{2} = e^{\frac{u_i}{2}} \sinh \frac{L_{ij}}{2} e^{\frac{u_j}{2}},$$

where L_{ij} is the initial edge length.

As shown in Fig. 14 2nd row and 2nd column, the hyperideal tetrahedron has one hyperideal vertex and three ideal vertices. The top hyperideal vertex is cut by a hyperbolic plane, the section is a hyperbolic triangle with edge lengths l_{ij} , l_{jk} and l_{ki} . The three ideal vertices are cut by horospheres, such that the "vertical" edge lengths are $-u_i$, $-u_j$ and $-u_k$ respectively. Furthermore, the bottom edge lengths are λ_{ij} , λ_{jk} and λ_{ki} respectively, where

$$\lambda_{ij} = 2 \log \sinh \frac{L_{ij}}{2} = \log 2\eta_{ij}.$$

Virtual radius Circle Packing. In this scheme ϵ is -1 , $\eta_{ij} > 0$, The edge length is given by

$$\cosh l_{ij} = \frac{\eta_{ij} \sinh r_i \sinh r_j + 1}{\cosh r_i \cosh r_j}.$$

As shown in Fig. 14 3rd row and 2nd column, the hyperbolic tetrahedron has one hyperideal vertex and three vertices inside \mathbb{H}^3 . The top hyperideal vertex is cut by a hyperbolic plane, the section is a hyperbolic triangle with edge lengths l_{ij} , l_{jk} and l_{ki} . The "vertical" edge lengths are $-u_i$, $-u_j$ and $-u_k$ respectively. Furthermore, the bottom edge lengths are λ_{ij} , λ_{jk} and λ_{ki} respectively, where

$$\cosh \lambda_{ij} = \eta_{ij}.$$

Remark 5.1. Similar to the Euclidean case, there is the mixed type hyperbolic scheme. The energy function relates to a truncated hyperbolic tetrahedron. Its top vertex is hyperideal. Its three bottom vertices are determined by the types ϵ_i, ϵ_j and ϵ_k .

5.3. Spherical background geometry. The general principle to obtain formula in spherical geometry, we only need to change \sinh and \cosh in hyperbolic geometry into \sin and \cos . Given a circle packing metric $(\Sigma, \gamma, \eta, \epsilon)$ with spherical background geometry, the length of an edge $[v_i, v_j]$ is

$$\cos l_{ij} = \frac{-4\eta_{ij}e^{u_i+u_j} + (1 - \epsilon_i e^{2u_i})(1 - \epsilon_j e^{2u_j})}{(1 + \epsilon_i e^{2u_i})(1 + \epsilon_j e^{2u_j})},$$

where $u_i = \log \tan \frac{\gamma_i}{2}$. The Hessian of the energy or the Jacobian has exactly the same formula as hyperbolic case

$$\frac{\partial(\theta_i, \theta_j, \theta_k)}{\partial(u_i, u_j, u_k)} = -\frac{1}{2A}L\Theta L^{-1}D,$$

where A and L is similar to those in Eqn. 5.4 and Eqn. 5.5 with $s(x) = \sin x$, Θ is the same as in Eqn. 5.6, and D is similar to that in Eqn. 5.7 with

$$\tau(i, j, k) = \cos l_i \cos^{\epsilon_j} \gamma_j - \cos^{\epsilon_k} \gamma_k.$$

Inversive Distance Circle Packing. The tangential and Thurston's circle packings can be unified as inversive distance circle packing. In this scheme ϵ is $+1$, $\eta_{ij} > 0$, the length is given by

$$\cos l_{ij} = \eta_{ij} \sin \gamma_i \sin \gamma_j + \cos \gamma_i \cos \gamma_j.$$

As shown in Fig. 14 1st row and 3rd column, the top vertex of the hyperbolic tetrahedron is inside \mathbb{H}^3 , with three corner angles l_{ij}, l_{jk} and l_{ki} . The other three hyperideal vertices are cut by three hyperbolic planes, such that the "vertical" edge lengths are $-u_i, -u_j$ and $-u_k$ respectively. The bottom lengths are $\lambda_{ij}, \lambda_{jk}$ and λ_{ki} respectively, where

$$\cosh \lambda_{ij} = \eta_{ij}.$$

Yamabe Flow. In this scheme ϵ is 0 , $\eta_{ij} > 0$, The edge length is given by

$$\sin \frac{l_{ij}}{2} = e^{\frac{u_i}{2}} \sin \frac{L_{ij}}{2} e^{\frac{u_j}{2}},$$

where L_{ij} is the initial edge length.

As shown in Fig. 14 2nd row and 3rd column, the top vertex of the hyperbolic tetrahedron is inside \mathbb{H}^3 , with three corner angles l_{ij}, l_{jk} and l_{ki} . The other three ideal vertices are cut by three horospheres, such that the "vertical" edge lengths are $-u_i, -u_j$ and $-u_k$ respectively. The bottom lengths are $\lambda_{ij}, \lambda_{jk}$ and λ_{ki} respectively, where

$$\lambda_{ij} = \log 2\eta_{ij}.$$

Virtual radius Circle Packing. In this scheme ϵ is -1 , $\eta_{ij} > 0$, The edge length is given by

$$\cos l_{ij} = \frac{\eta_{ij} \sin \gamma_i \sin \gamma_j + 1}{\cos \gamma_i \cos \gamma_j}.$$

As shown in Fig. 14 3rd row and 3rd column, the hyperbolic tetrahedron has all four vertices inside \mathbb{H}^3 . The top vertex is with three corner angles l_{ij}, l_{jk} and

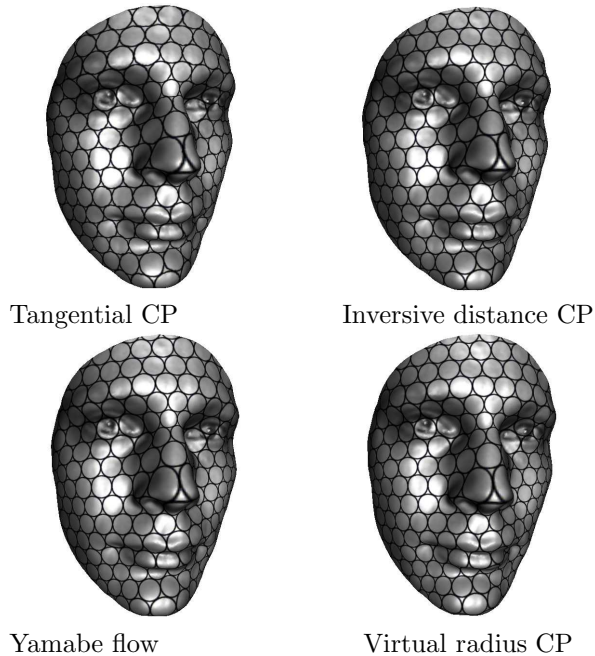


FIGURE 11. Conformality test for different schemes.

l_{ki} , the “vertical” edge lengths are $-u_i$, $-u_j$ and $-u_k$ respectively. The bottom lengths are λ_{ij} , λ_{jk} and λ_{ki} respectively, where

$$\cosh \lambda_{ij} = \eta_{ij}.$$

Remark 5.2. Similar to \mathbb{E}^2 and \mathbb{H}^2 cases, there is the mixed type for \mathbb{S}^2 case. The energy function relates to a truncated hyperbolic tetrahedron. Its top vertex is in \mathbb{H}^3 . Its three bottom vertices are determined by the types ϵ_i , ϵ_j and ϵ_k .

6. EXPERIMENTAL RESULTS

Our current implementation covers all schemes: Thurston’s circle packing, tangential circle packing, inversive distance circle packing, Yamabe flow and virtual radius circle packing, for discrete surfaces with Euclidean and Hyperbolic background geometries. The algorithms can handle surfaces with different topologies. The package is accessible for the whole research community. The geometric data sets are from the public databases, such as [1] and [2]. The human face surfaces were scanned from a high speed and high resolution, phase shifting scanner, as described in [38]. We tested our algorithm on a huge amount of various models, including different sizes and topology types.

Generality. Fig. 1 and Fig. 3 demonstrate the generality of Ricci flow method to handle surfaces with all possible topologies. These two figures cover all the topology types of compact surfaces.

Conformality. Fig. 12 and Fig. 11 compares the qualities of different schemes. In general, tangential circle packing scheme assumes all the edges lengths to be

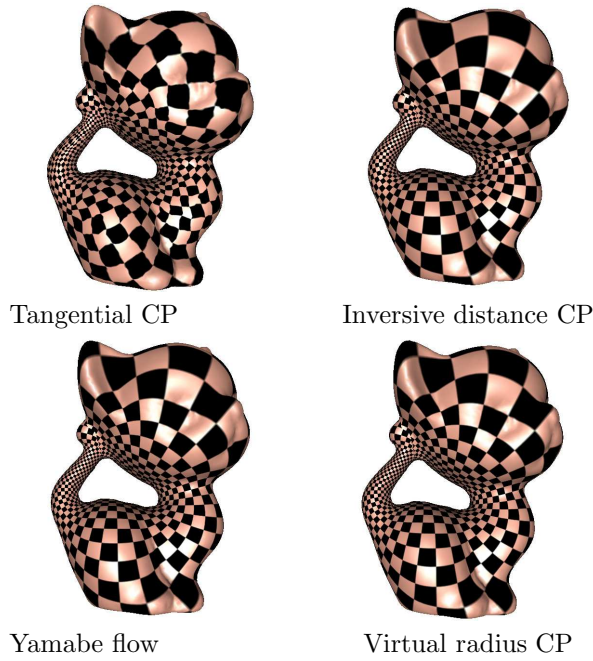


FIGURE 12. Conformality test for different schemes.

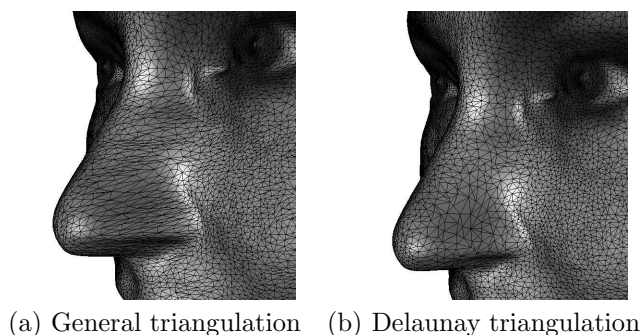
one, therefore the conformality is as good as other schemes. On the other hand, tangential circle packing scheme is robust to low qualities meshes.

Robustness. We also test robustness to the mesh qualities of different schemes. As shown in Fig. 13, we use different schemes to compute Riemann mapping. For low quality meshes, the tangential circle packing scheme outperforms others. If we allow the connectivity to be modified during the flow, then all schemes succeed on both surfaces.

7. CONCLUSION

This work establishes a unified framework for discrete surface Ricci flow, which covers most existing schemes: tangential circle packing, Thurston's circle packing, inversive distance circle packing, discrete Yamabe flow, virtual radius circle packing and mixed scheme, with Spherical, Euclidean and hyperbolic background geometry. For the first time, two novel schemes, virtual radius circle packing and the mixed scheme, are introduced. This work also gives explicit geometric interpretation to the discrete Ricci energy for all the schemes, and Hessian of the discrete Ricci energy for schemes with Euclidean background geometry.

The unified frame work deepen our understanding to the the discrete surface Ricci flow theory, and inspired us to discover the novel schemes of virtual radius circle packing and the mixed scheme, improved the flexibility and robustness of the algorithms, greatly simplified the implementation and improved the debugging efficiency. Experimental results show the unified surface Ricci flow algorithms can handle surfaces with all possible topologies, and are robust to meshes with different qualities, and effective for solving real problems.



(a) General triangulation (b) Delaunay triangulation

FIGURE 13. The input meshes for the robustness tests.

In the future, we will focus on parallel algorithms for surface Ricci flow and prove the convergence of discrete Ricci flow to the smooth Ricci flow.

REFERENCES

- [1] The digital michelangelo project. <https://graphics.stanford.edu/projects/mich/>.
- [2] Repository of aim@shape project. <http://shapes.aimatshape.net/>.
- [3] E. M. Andreev. Complex polyhedra in Lobachevsky spaces. (*Russian*) *Mat. Sb. (N.S.)*, 81(123):445–478, 1970.
- [4] E. M. Andreev. Convex polyhedra of finite volume in Lobachevsky space. (*Russian*) *Mat. Sb. (N.S.)*, 83(125):256–260, 1970.
- [5] A. I. Bobenko and B. A. Springborn. Variational principles for circle patterns and Koebe’s theorem. *Trans. Amer. Math. Soc.*, 356(2):659–689, 2004.
- [6] P. L. Bowers and K. Stephenson. Uniformizing dessins and Belyi maps via circle packing. *Mem. Amer. Math. Soc.*, 170(805), 2004.
- [7] S. Chern. An elementary proof of the existence of isothermal parameters on a surface. *Proceedings of the American Mathematical Society*, 6(5):771–782, October 1955.
- [8] B. Chow. The Ricci flow on the 2-sphere. *Journal of Differential Geometry*, 33(2):325–334, 1991.
- [9] B. Chow, P. Lu, and L. Ni. *Hamilton’s Ricci Flow*, volume 77 of *Graduate Studies in Mathematics*. AMS, 2006.
- [10] B. Chow and F. Luo. Combinatorial Ricci flows on surfaces. *Journal Differential Geometry*, 63(1):97–129, 2003.
- [11] Y. C. de Verdière. Un principe variationnel pour les empilements de cercles. *Invent. Math.*, 104:655–669, 1991.
- [12] D. Glickenstein. A combinatorial Yamabe flow in three dimensions. *Topology*, 44(4):791–808, 2005.
- [13] D. Glickenstein. A maximum principle for combinatorial Yamabe flow. *Topology*, 44(4):809–825, 2005.
- [14] D. Glickenstein. Discrete conformal variations and scalar curvature on piecewise flat two and three dimensional manifolds. *Journal of Differential Geometry*, 87(2):201–238, 2011.
- [15] X. Gu, Y. He, M. Jin, F. Luo, H. Qin, and S.-T. Yau. Manifold splines with a single extraordinary point. *Computer-Aided Design*, 40(6):676–690, 2008.
- [16] X. Gu, F. Luo, J. Sun, and T. Wu. A discrete uniformization theorem for polyhedral surfaces. *arXiv:1309.4175*, pages 1–13, Feb 2013.
- [17] G. Guennebaud, B. Jacob, et al. Eigen. <http://eigen.tuxfamily.org>, 2010.
- [18] R. Guo. Combinatorial Yamabe flow on hyperbolic surfaces with boundary. *Communications in Contemporary Mathematics*, 13(5):827–842, 2011.
- [19] R. Guo. Local rigidity of inversive distance circle packing. *Trans. Amer. Math. Soc.*, 363:4757–4776, 2011.
- [20] R. Guo and F. Luo. Rigidity of polyhedral surface ii. *Geom. Topol.*, 13:1265–1312, 2009.

- [21] R. Hamilton. Ricci flow on surfaces. *Mathematics and General Relativity, Contemporary Mathematics AMS, Providence, RI.*, 71:237–261, 1988.
- [22] Z.-X. He and O. Schramm. On the convergence of circle packings to the Riemann map. *Invent. Math.*, 125:285–305, 1996.
- [23] M. Jin, J. Kim, F. Luo, and X. Gu. Discrete surface Ricci flow. *IEEE Transactions on Visualization and Computer Graphics*, 14(5):1030–1043, 2008.
- [24] P. Koebe. Kontaktprobleme der konformen abbildung. *Ber. Sächs. Akad. Wiss. Leipzig, Math. Phys. Kl.*, 88:141–164, 1936.
- [25] G. Leibon. Characterizing the Delaunay decompositions of compact hyperbolic surface. *Geom. Topol.*, 6:361–391, 2002.
- [26] F. Luo. Combinatorial Yamabe flow on surfaces. *Contemp. Math.*, 6(5):765–780, 2004.
- [27] F. Luo. Rigidity of polyhedral surfaces. *arXiv:math.GT/0612714*, 2006.
- [28] F. Luo. Rigidity of polyhedral surfaces, iii. *Geometry and Topology*, 15(4):2299–2319, December 2011.
- [29] F. Luo, X. Gu, and J. Dai. *Variational Principles for Discrete Surfaces*. Advanced Lectures in Mathematics. High Education Press and International Press, 2007.
- [30] A. Marden and B. Rodin. *Computational methods and function theory (Valpara’iso,1989)*, volume 1435 of *Lecture Notes in Math.*, chapter On Thurston’s formulation and proof of Andreev’s theorem, pages 103–116. Springer, Berlin, 1990.
- [31] I. Rivin. Euclidean structures of simplicial surfaces and hyperbolic volume. *Ann. of Math.*, 139:553–580, 1994.
- [32] B. Rodin and D. Sullivan. The convergence of circle packings to the Riemann mapping. *Journal of Differential Geometry*, 26:349–360, 1987.
- [33] R. Schoen and S.-T. Yau. *Lecture on Differential Geometry*, volume 1. International Press Incorporated, Boston, 1994.
- [34] B. Springborn. A variational principle for weighted Delaunay triangulation and hyperideal polyhedra. *Journal of Differential Geometry*, 78(2):333–367, 2008.
- [35] B. Springborn, P. Schröder, and U. Pinkall. Conformal equivalence of triangle meshes. *ACM Trans. Graph.*, 27(3):1–11, 2008.
- [36] K. Stephenson. *Introduction to Circle Packing: The Theory of Discrete Analytic Functions*. Cambridge University Press, 2005.
- [37] W. P. Thurston. *The Geometry and Topology of 3-manifolds*. Princeton University Press, 1981.
- [38] Y. Wang, M. Gupta, S. Zhang, S. Wang, X. Gu, D. Samaras, and P. Huang. High resolution tracking of non-rigid motion of densely sampled 3d data using harmonic maps. *International Journal of Computer Vision*, 76(3):283–300, 2008.
- [39] W. Brägger. Kreispackungen und triangulierugen. *Enseign. Math.*, 38:201–217, 1992.
- [40] W. Zeng, J. Marino, K. Gurijala, X. Gu, and A. Kaufman. Supine and prone colon registration using quasi-conformal mapping. *IEEE Transactions on Visualization and Computer Graphics*, 16(6):1348–1357, 2010.
- [41] W. Zeng, D. Samaras, and X. D. Gu. Ricci flow for 3D shape analysis. *IEEE Transactions on Pattern Analysis and Machine Intelligence*, 32(4):662–677, 2010.

APPENDIX

In the appendix, we explain the unified surface Ricci flow algorithm 1 in details, and reorganize all the formulae necessary for the coding purpose.

Step 1. Initial Circle Packing (γ, η) . Depending on different schemes, the initialization of the circle packing is different. The mesh has induced Euclidean metric l_{ij} . For inversive distance circle packing, we choose

$$\gamma_i = \frac{1}{3} \min_j l_{ij},$$

this ensures all the vertex circles are separated. For Yamabe flow, we choose all γ_i to be 1. For virtual radius circle packing, we choose all γ_i ’s to be 1. Then γ_{ij} can be computed using the l_{ij} formula in Tab. 1.

Algorithm 1 Unified Surface Ricci Flow**Require:** The inputs include:

1. A triangular mesh Σ , embedded in \mathbb{E}^3 ;
2. The background geometry, \mathbb{E}^2 , \mathbb{H}^2 or \mathbb{S}^2 ;
3. The circle packing scheme, $\epsilon \in \{+1, 0, -1\}$;
4. A target curvature \bar{K} , $\sum \bar{K}_i = 2\pi\chi(\Sigma)$ and $\bar{K}_i \in (-\infty, 2\pi)$.

Ensure: A discrete metric conformal to the original one, which realizes the target curvature \bar{K} .

- 1: Initialize the circle radii γ , discrete conformal factor u and conformal structure coefficient η , obtain the initial circle packing metric $(\Sigma, \gamma, \eta, \epsilon)$
- 2: **while** $\max_i |\bar{K}_i - K_i| > \text{threshold}$ **do**
- 3: Compute the circle radii γ from the conformal factor u
- 4: Compute the edge length from γ and η
- 5: Compute the corner angle θ_i^{jk} from the edge length using cosine law
- 6: Compute the vertex curvature K
- 7: Compute the Hessian matrix H
- 8: Solve linear system $H\delta u = \bar{K} - K$
- 9: Update conformal factor $u \leftarrow u - \delta u$
- 10: **end while**
- 11: Output the result circle packing metric.

	u_i	Edge Length l_{ij}	$\tau(i, j, k)$	$s(x)$
\mathbb{E}^2	$\log \gamma_i$	$l_{ij}^2 = 2\eta_{ij}e^{u_i+u_j} + \epsilon_i e^{2u_i} + \epsilon_j e^{2u_j}$	$\frac{1}{2}(l_i^2 + \epsilon_j \gamma_j^2 - \epsilon_k \gamma_k^2)$	x
\mathbb{H}^2	$\log \tanh \frac{\gamma_i}{2}$	$\cosh l_{ij} = \frac{4\eta_{ij} + (1 + \epsilon_i e^{2u_i})(1 + \epsilon_j e^{2u_j})}{(1 - \epsilon_i e^{2u_i})(1 - \epsilon_j e^{2u_j})}$	$\cosh l_i \cosh^{\epsilon_j} \gamma_j - \cosh^{\epsilon_k} \gamma_k$	$\sinh x$
\mathbb{S}^2	$\log \tan \frac{\gamma_i}{2}$	$\cosh l_{ij} = \frac{4\eta_{ij} + (1 - \epsilon_i e^{2u_i})(1 - \epsilon_j e^{2u_j})}{(1 + \epsilon_i e^{2u_i})(1 + \epsilon_j e^{2u_j})}$	$\cos l_i \cos^{\epsilon_j} \gamma_j - \cos^{\epsilon_k} \gamma_k$	$\sin x$

TABLE 1. Formulae for \mathbb{E}^2 , \mathbb{H}^2 and \mathbb{S}^2 background geometries.

Step 3. Circle Radii γ . The computation for circle radii from conformal factor uses the formulae in the first column in Tab.1.

Step 4. Edge Length l . The computation of edge lengths from conformal factor u and conformal structure coefficient η uses the formulae in the 2nd column in Tab.1

Step 5. Corner Angle θ . The computation from edge length l to the corner angle θ uses the cosine law formulae,

$$\begin{aligned}
l_k^2 &= l_i^2 + l_j^2 - 2l_i l_j \cos \theta_k & \mathbb{E}^2 \\
\cosh l_k &= \cosh l_i \cosh l_j - \sinh l_i \sinh l_j \cos \theta_k & \mathbb{H}^2 \\
\cos l_k &= \cos l_i \cos l_j - \sin l_i \sin l_j \cos \theta_k & \mathbb{S}^2
\end{aligned}$$

Step 6. Vertex Curvature K . The vertex curvature is defined as angle deficit

$$K(v_i) = \begin{cases} 2\pi - \sum_{[v_i, v_j, v_k]} \theta_i^{jk} & v_i \notin \partial\Sigma \\ \pi - \sum_{[v_i, v_j, v_k]} \theta_i^{jk} & v_i \in \partial\Sigma \end{cases}$$

Step 7. Hessian Matrix H .

$$\frac{\partial(\theta_i, \theta_j, \theta_k)}{\partial(u_i, u_j, u_k)} = -\frac{1}{2A} L \Theta L^{-1} D,$$

where

$$A = \sin \theta_i s(l_j) s(l_k),$$

and

$$L = \text{diag}(s(l_i), s(l_j), s(l_k)),$$

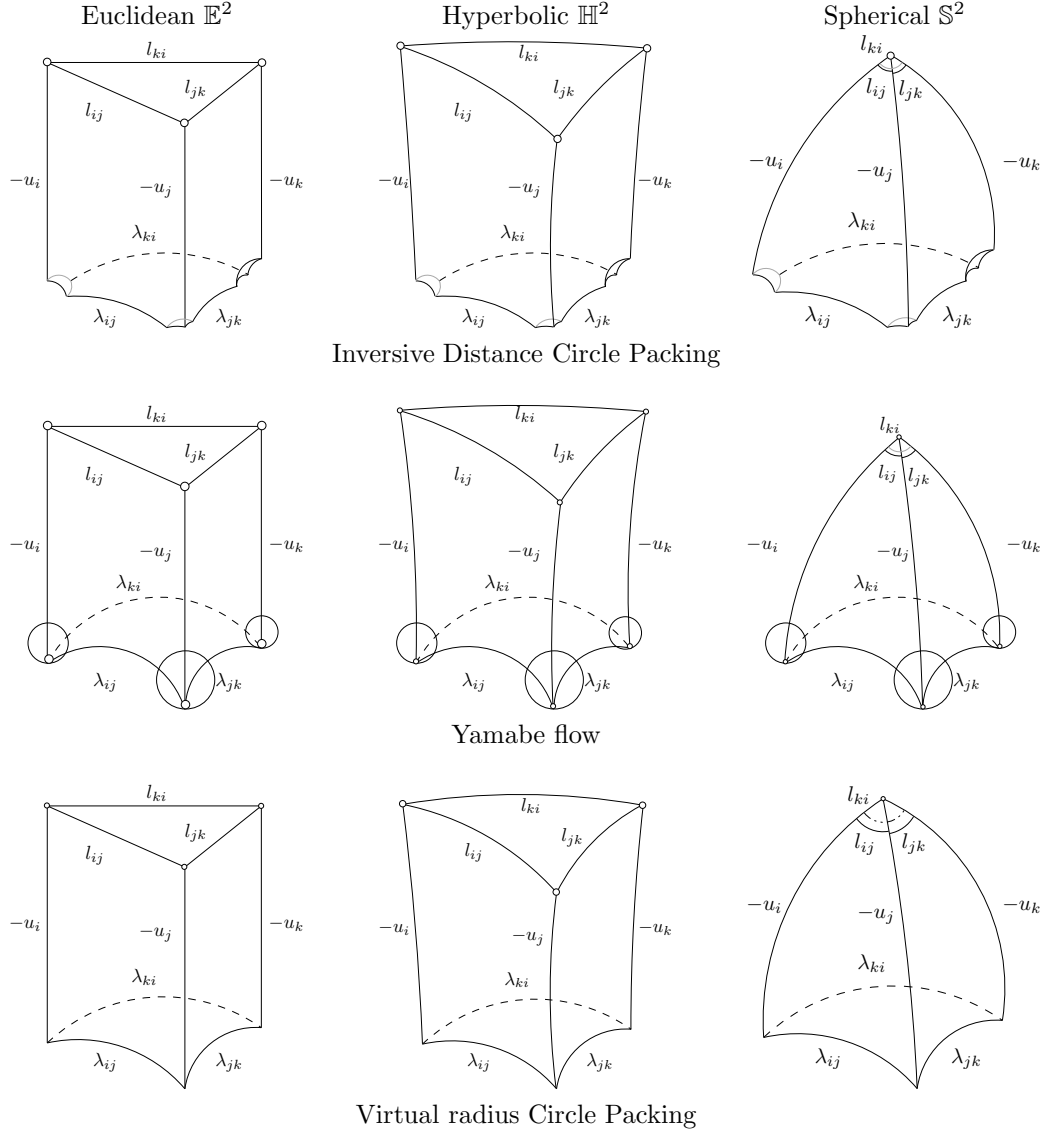


FIGURE 14. Geometric meaning of discrete Ricci energy - volumes of truncated hyperbolic tetrahedra.

and

$$D = \begin{pmatrix} 0 & \tau(i, j, k) & \tau(i, k, j) \\ \tau(j, i, k) & 0 & \tau(j, k, i) \\ \tau(k, i, j) & \tau(k, j, i) & 0 \end{pmatrix}.$$

Step. 8 Linear System. If the Σ is with \mathbb{H}^2 background geometry, then the Hessian matrix H is positive definite; else if Σ is with \mathbb{E}^2 background geometry, then H is positive definite on the linear subspace $\sum_i u_i = 0$. The linear system can be solved using any sparse linear solver, such as Eigen [17].

Remark 7.1. For discrete surface Ricci flow with topological surgeries, we can add one more step right after step 4. In this new step, we modify the connectivity of Σ to keep the triangulation to be (Power) Delaunay.

Remark 7.2. In Alg. 1, ϵ is a constant function defined on the vertices. The algorithm can be easily modified for mixed type scheme with \mathbb{E}^2 , \mathbb{H}^2 and \mathbb{S}^2 background geometries, by changing ϵ to be a non-constant function with values in $\{-1, 0, +1\}$.

MIN ZHANG, DEPARTMENT OF COMPUTER SCIENCE,

STATE UNIVERSITY OF NEW YORK AT STONY BROOK, NY 11794, USA

E-mail address: `mzhang@cs.sunysb.edu`

REN GUO, DEPARTMENT OF MATHEMATICS,

OREGON STATE UNIVERSITY, OR 97331, USA

E-mail address: `guore@math.oregonstate.edu`

WEI ZENG, SCHOOL OF COMPUTING AND INFORMATION SCIENCES,

FLORIDA INTERNATIONAL UNIVERSITY, FL 33199, USA

E-mail address: `wzeng@cs.fiu.edu`

FENG LUO, DEPARTMENT OF MATHEMATICS,

RUTGERS UNIVERSITY, NJ 08854, USA

E-mail address: `fluo@math.rutgers.edu`

SHING-TUNG YAU, DEPARTMENT OF MATHEMATICS,

HARVARD UNIVERSITY, MA 02138, USA

E-mail address: `yau@math.harvard.edu`

XIANFENG GU, DEPARTMENT OF COMPUTER SCIENCE,

STATE UNIVERSITY OF NEW YORK AT STONY BROOK, NY 11794, USA

E-mail address: `gu@cs.sunysb.edu`